Biomaterials Science

PAPER

View Article Online
View Journal | View Issue

Cite this: *Biomater. Sci.*, 2018, **6**, 614

Protein-engineered hydrogels enhance the survival of induced pluripotent stem cell-derived endothelial cells for treatment of peripheral arterial disease†

Abbygail A. Foster,[a,b] Ruby E. Dewi,[a] Lei Cai,[a] Luqia Hou,[b,c] Zachary Strassberg,[c] Cynthia A. Alcazar,[c] Sarah C. Heilshorn [a,b] and Ngan F. Huang *[b,c,d]

Received 28th September 2017,
Accepted 23rd January 2018

DOI: 10.1039/c7bm00883j

rsc.li/biomaterials-science

A key feature of peripheral arterial disease (PAD) is damage to endothelial cells (ECs), resulting in lower limb pain and restricted blood flow. Recent preclinical studies demonstrate that the transplantation of ECs *via* direct injection into the affected limb can result in significantly improved blood circulation. Unfortunately, the clinical application of this therapy has been limited by low cell viability and poor cell function. To address these limitations we have developed an injectable, recombinant hydrogel, termed SHIELD (Shear-thinning Hydrogel for Injectable Encapsulation and Long-term Delivery) for cell transplantation. SHIELD provides mechanical protection from cell membrane damage during syringe flow. Additionally, secondary *in situ* crosslinking provides a reinforcing network to improve cell retention, thereby augmenting the therapeutic benefit of cell therapy. In this study, we demonstrate the improved acute viability of human induced pluripotent stem cell-derived endothelial cells (iPSC-ECs) following syringe injection delivery in SHIELD, compared to saline. Using a murine hind limb ischemia model of PAD, we demonstrate enhanced iPSC-EC retention *in vivo* and improved neovascularization of the ischemic limb based on arteriogenesis following transplantation of iPSC-ECs delivered in SHIELD.

Introduction

Peripheral arterial disease (PAD) is a highly prevalent vascular disease that affects approximately 202 million adults worldwide.[1] PAD patients suffer from ischemia due to narrowing of the arteries, resulting in impaired oxygen delivery and tissue loss.[2] Current surgical interventions such as angioplasty or bypass surgery target the primary occluded macro vessel. Unfortunately, these approaches fail to reverse or treat the surrounding microvasculature, often leading to irreversible tissue loss and potential limb amputation.[3] Cell transplantation into the ischemic tissue has emerged as a novel therapeutic strategy to re-establish functional collateral networks that supply oxygenated blood and preserve tissue viability.[4,5] For example, human induced pluripotent stem cell-derived endothelial cells (iPSC-ECs) injected into the ischemic calf muscle in a murine hind limb ischemia (HLI) model of PAD have shown enhanced microvascular density and improved blood reperfusion.[6] These cells are thought to facilitate tissue regeneration by secreting angiogenic cytokines and incorporating into expanding endogenous microvasculature.[7] While these data are encouraging, the clinical adoption of iPSC-EC therapy is currently hampered by the rapid decline in the viability of transplanted cells, which requires multiple, sequential cell injections to achieve therapeutic efficacy.

To overcome the limitation of transplanted cell death, we have designed an injectable material to improve cell viability and promote greater therapeutic neovascularization after a single administration of iPSC-ECs. This material must overcome both short-term and long-term challenges to cell viability to improve the potential clinical success of single-dose iPSC-EC transplantation. First, during the transplantation process, the number of viable cells plummets during injection due to membrane damaging extensional forces experienced in the syringe needle.[8] Second, injectable cell therapies often result in low long-term cell retention and proliferation at the site of injection due to the lack of appropriate endogenous cues, limiting their therapeutic function.[9,10] We hypothesized that a three-dimensional (3D) injectable hydrogel with

[a]*Department of Materials Science and Engineering, Stanford University, Stanford, CA, USA*
[b]*Stanford Cardiovascular Institute, Stanford University, Stanford, CA, USA. E-mail: ngantina@stanford.edu*
[c]*Veterans Affairs Palo Alto Health Care System, Palo Alto, CA, USA*
[d]*Department of Cardiothoracic Surgery, Stanford, CA, USA*

†Electronic supplementary information (ESI) available. See DOI: 10.1039/c7bm00883j

dynamic control of mechanical properties would address both these challenges by providing (1) acute mechanical protection to iPSC-ECs during injection and (2) long-term mechanical cues to promote the iPSC-EC retention and pro-angiogenic secretory profile after injection.

Current clinical protocols using low viscosity fluids such as saline for cell transplantation into solid tissue may cause substantial cell death due to high mechanical forces and subsequent cell membrane damage during the injection process.[8,10] Preclinical studies of injection have demonstrated that cell transplantation using shear-thinning hydrogels can provide acute protection from this membrane damage by encapsulating the cells within a hydrogel that shields the cells from these mechanical forces.[11–13] Following injection into the ischemic tissue, the cells are confronted with additional survival challenges including hypoxia and local inflammatory responses. Recent preclinical studies have shown that the mechanical microenvironment can influence cell proliferation,[14,15] migration,[16,17] and growth factor secretion,[18,19] which may assist cell survival and function at the transplantation site. Based on these previous studies, we hypothesized that a two-stage, shear-thinning hydrogel could first provide mechanical protection during cell transplantation by syringe injection and then provide mechanical cues to promote cell retention and secretion of pro-angiogenic cues following injection.

We previously designed an injectable hydrogel termed SHIELD (shear-thinning hydrogel for injectable encapsulation and long-term delivery) and reported proof-of-concept data that this material enhanced the subcutaneous transplantation of adipose-derived stem cells (ASCs) into healthy mice.[20] Here we report the first use of this novel family of biomaterials in a preclinical disease model, demonstrating iPSC-EC transplantation as a regenerative therapy for PAD. Specifically, we modulated the *in situ* stiffness of the hydrogel to span the range from 10 to 1000 Pa and identified those materials that protected encapsulated iPSC-ECs from damaging injection forces and hypoxia. Each of these SHIELD variants used heterodimeric peptide assembly to form weak gels *ex situ* and also contained varying concentrations of a thermo-responsive polymer to provide a tunable amount of secondary stiffening *in situ*. This hydrogel was co-delivered with iPSC-ECs in a murine hind limb ischemia (HLI) model of PAD to evaluate transplanted iPSC-EC viability and regenerate collateral microvessel density. Together, these data suggest that SHIELD can improve the regenerative potential of a single dose of transplanted iPSC-ECs by providing acute protection against membrane damage during injection and providing a stable matrix *in situ* to support cell viability, pro-angiogenic factor secretion after injection, and neovascularization.

Results & discussion

Tuning SHIELD *in situ* mechanical properties

We hypothesized that an injectable hydrogel with dynamic control of mechanical properties would improve iPSC-EC therapeutic potential by providing both mechanical protection to iPSC-ECs during injection and mechanical cues to promote iPSC-EC proliferation and pro-angiogenic factor secretion after injection. To accomplish this dynamic control of mechanics, we developed the SHIELD material to undergo two distinct cross-linking stages (Fig. 1A). In the first stage, an engineered recombinant protein (C7) and a multi-armed, P1-peptide-modified polyethylene glycol (PEG) assemble by heterodimeric binding of peptide domains C and P to form a weak gel. The recombinant protein C7 facilitates physical crosslinking of SHIELD to provide mechanical protection to encapsulated cells and maintains cell-matrix adhesions through integrin binding of RGD cell-binding domains to promote the survival of the encapsulated iPSC-ECs. In the second stage, a thermal phase transition of thermoresponsive poly(*N*-isopropylacrylamide) (PNIPAM), with lower critical solution temperature (LCST) of 32 °C, provides secondary crosslinking *in situ* to stiffen the hydrogel network.

To demonstrate sol–gel phase transition upon mixing of the individual liquid components, we ejected individual or pre-mixed SHIELD components onto vertical glass slides (Fig. 1B). When ejected, the individual components flowed as liquids, covering the length of the slide in 10 s. In contrast, after the two components were simply mixed together to form SHIELD, the resulting gel resisted flow due to hetero-

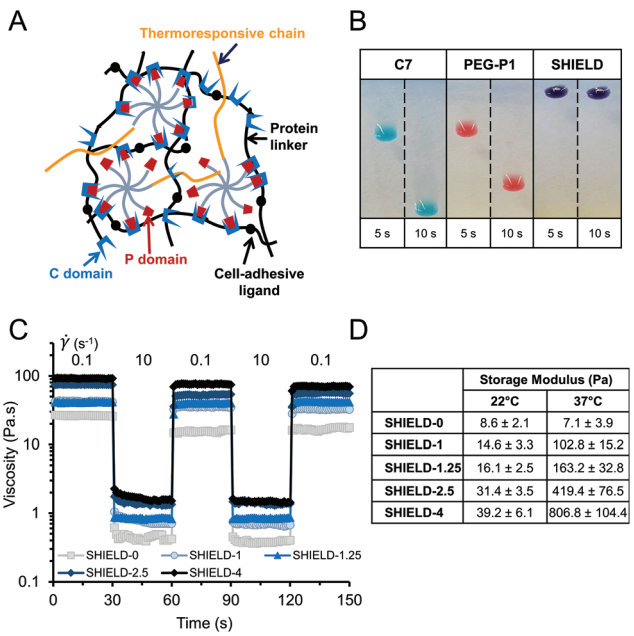

	Storage Modulus (Pa)	
	22°C	37°C
SHIELD-0	8.6 ± 2.1	7.1 ± 3.9
SHIELD-1	14.6 ± 3.3	102.8 ± 15.2
SHIELD-1.25	16.1 ± 2.5	163.2 ± 32.8
SHIELD-2.5	31.4 ± 3.5	419.4 ± 76.5
SHIELD-4	39.2 ± 6.1	806.8 ± 104.4

Fig. 1 Shear thinning hydrogel design and characterization. (A) Schematic of SHIELD, which is formed by mixing together two components: C7 engineered protein and 8-arm PEG-P1 with or without thermoresponsive PNIPAM. (B) Ejection of the SHIELD components C7 and PEG-P1 either alone or after mixing together to form a gel onto an inclined glass slide. (C) Shear-thinning and self-healing properties of SHIELD under alternating shear rates of 0.1 and 10 s^{-1} at 22 °C. (D) Storage (G') moduli of SHIELD formulations with varying PNIPAM contents at 22 °C and 37 °C ($n \geq 3$).

dimeric peptide binding between the two components at room temperature.

The bulk mechanical properties of SHIELD were tuned by varying the molecular weight (M_w) and weight percentage (wt%) of PNIPAM as previously reported[19,20] to obtain a family of injectable hydrogels. We next evaluated the shear-thinning properties of these hydrogels during high-shear flow, such as that experienced during syringe injection. SHIELD hydrogel viscosity was assessed at alternating low and high shear rates (0.1 and 10 s^{-1} respectively). When subjected to high shear rates, the viscosity rapidly decreased (<1 s) to ≈0.5–2 Pa s (Fig. 1C). When low shear rates were applied, the materials rapidly self-healed (<1 s) to achieve the original hydrogel viscosity of ≈20–100 Pa s. All hydrogels demonstrated fully reversible shear-thinning and self-healing behavior across multiple cycles.

Additional oscillatory rheological studies confirmed that these materials form robust gels with *in situ* shear storage moduli (G') spanning two orders of magnitude at body temperature (Fig. 1D). At room temperature, all SHIELD formulations had relatively similar stiffness (G' ≈10–40 Pa), allowing for easy hand injection. As anticipated, the stiffness of SHIELD-0 (with 0 wt% PNIPAM) remained constant following an increase in temperature to 37 °C. In contrast, the stiffness of SHIELD-1 (with 1 wt% PNIPAM) increased tenfold to ≈100 Pa due to the thermal phase transition of PNIPAM. This stiffening effect was further increased as the PNIPAM wt% was increased, with G' ≈ 1000 Pa for SHIELD-4. Together these data demonstrate that SHIELD hydrogels form weak, reversible networks at room temperature and undergo thermoresponsive secondary crosslinking upon *in situ* warming.

SHIELD improves acute post-injection viability of iPSC-ECs *in vitro*

We hypothesized that encapsulation in a weak hydrogel would facilitate enhanced iPSC-EC acute viability compared to cell delivery in PBS alone due to the cell protective capabilities of shear-thinning hydrogels.[8,9] Thus, we evaluated iPSC-EC acute membrane damage following *in vitro* cell encapsulation and injection. The iPSC-ECs were encapsulated in various SHIELD formulations within a 1 mL syringe barrel prior to ejection through a 28 G syringe needle. The cells were analyzed for acute membrane damage using a non-membrane-permeable dye, ethidium homodimer. Viable cells with intact membranes were visualized with a membrane-permeable, enzyme-activated dye, calcein AM (Fig. 2A). Our results show that iPSC-EC encapsulation in SHIELD provided significant protection from acute membrane damage. After injection, 34 ± 9% of iPSC-ECs delivered with PBS exhibited membrane damage. In contrast, for all SHIELD formulations tested, less than 10% iPSC-ECs suffered acute membrane damage, similar to non-injected controls (Fig. 2B). These results suggest that the weak gel network formed by heterodimeric peptide binding, which is present in all SHIELD formulations, provides significant cell protection from the damaging mechanical forces experienced during syringe injection. These data are consistent with previous reports for other cell types[20] and other materials[8,21,22] that demonstrate shear-thinning hydrogels can provide mechanical protection to cells during injection.

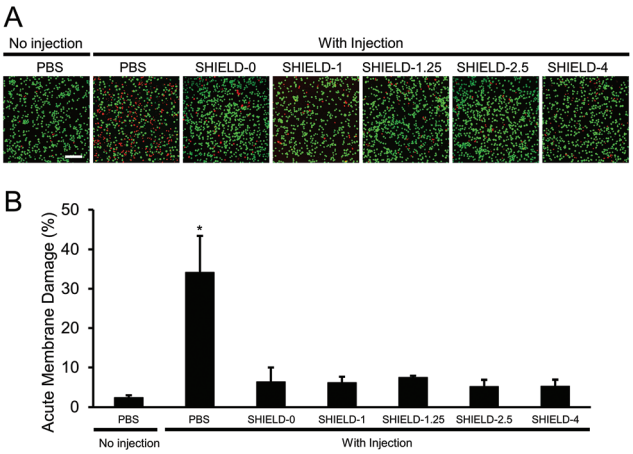

Fig. 2 Quantification of cell viability using live/dead cytotoxicity assay. (A) Fluorescence images of iPSC-ECs stained with LIVE/DEAD assay (green/red, respectively) within PBS or SHIELD immediately post-injection. (B) Acute membrane damage following *in vitro* injection through a 28 G syringe needle at 1.0 mL min^{-1}. *p < 0.05 compared to other treatment groups, n = 5. Scale bar: 200 μm.

SHIELD material properties modulate hypoxic proliferation rates

To better mimic the hypoxic conditions that transplanted cells experience in an ischemic limb, iPSC-ECs were injected as described into a cell culture mold and incubated in a hypoxic chamber (1% O_2) at physiological temperature to induce thermo-responsive stiffening of the gel network. The 3D cultures were maintained for up to 14 days post-injection. We quantified the cell number throughout the culture period to assess if SHIELD formulations could support cell proliferation in hypoxia. Our results indicated that the iPSC-ECs remained proliferative over 14 days of *in vitro* culture in SHIELD formulations with up to 2.5 wt% PNIPAM (Fig. 3A). Specifically, the quantification of the cell number indicated that proliferation is statistically greater within SHIELD-1.25 and SHIELD-2.5 compared to other formulations. The visualization of F-actin revealed a well-spread cytoskeletal morphology and distinct actin filament networks in SHIELD formulations with up to 2.5 wt% PNIPAM (Fig. 3B). SHIELD-4 did not support long-term cell proliferation or cell spreading. We previously demonstrated that increasing the PNIPAM secondary network density in SHIELD resulted in significantly slower diffusion, indicating a smaller mesh size for the double-network hydrogels.[20] The reduced cell spreading and proliferation in SHIELD-4 is potentially due to the presumably smaller mesh sizes in this hydrogel formulation, which may create a more restrictive microenvironment and prohibit iPSC-EC proliferation.[23] However, a limitation of this study is the inability to assess proliferation in a control 3D environment in the absence of SHIELD.

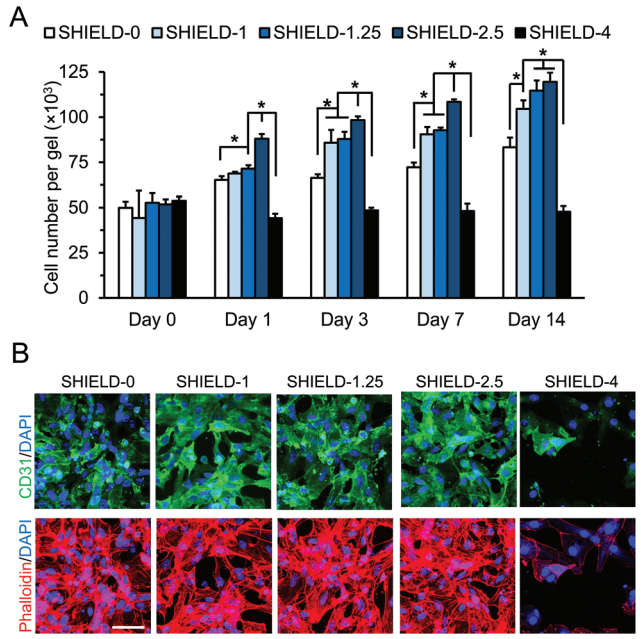

Fig. 3 Proliferation of iPSC-ECs within SHIELD in hypoxia. (A) DNA qualification at days 0, 1, 3, 7, and 14 post-injection. (B) Confocal 3D projection images of iPSC-ECs cultured within SHIELD at day 14 post-injection stained with CD31 (green)/DAPI (blue) and rhodamine phalloidin (red)/DAPI (blue). *$p < 0.05$, ($n \geq 3$). Scale bar: 50 μm.

Therefore, it is unclear how cell proliferation compares in the absence of this hydrogel.

iPSC-ECs encapsulated in SHIELD secrete paracrine factors that promote neovascularization

The secretion of paracrine and trophic factors is thought to play an important role in tissue recovery following an ischemic insult.[24,25] Several studies have delivered pro-angiogenic factors directly to the ischemic site to promote tissue recovery.[26–28] In addition, previous studies have demonstrated that *in vitro* exposure of iPSC-ECs to hypoxia resulted in an increased expression of various angiogenic cytokines and growth factors in 2D culture.[6] To investigate if 3D hydrogel culture would promote a pro-angiogenic secretory profile from encapsulated iPSC-ECs, the cells were injected into molds using SHIELD-0 and SHIELD-2.5. During normoxic culture, relatively similar levels of secretory release were observed for all selected pro-angiogenic factors regardless of cell encapsulation in SHIELD-0 or SHIELD-2.5. Higher levels of the hypoxia-induced chemoattractants endothelin-1 and IL-8 were detected in the conditioned media from iPSC-ECs cultured in hypoxia, compared to normoxia, for both hydrogel formulations in two independent antibody arrays (Fig. S1†). These results are consistent with previous reports demonstrating the increased expression of these chemoattractants in response to reduced oxygen tension.[29] In addition, the secretion of a urokinase-type plasminogen activator (uPA) increased in hypoxic culture using both SHIELD formulations, consistent with reports of increased uPA expression in human microvascular endothelial cells (HMVECs), and a subsequent increase in plasmin formation to stimulate tubulogenesis.[30] Our results are consistent with preclinical animal studies which suggest that endothelial cells can secrete paracrine factors in response to hypoxia to increase the density and perfusion of the microvasculature.[6,30,31]

SHIELD improves iPSC-EC survival and therapeutic efficacy in a murine model of PAD

Previous preclinical work demonstrated that the transplantation of iPSC-ECs with saline improved blood perfusion and re-vascularization of the ischemic limb in a rodent model of PAD.[6] However, iPSC-EC viability rapidly declined after transplantation, necessitating multiple cell administrations. We hypothesized that cell encapsulation in SHIELD would provide a minimally invasive and enduring therapy by providing acute protection during injection and promoting long-term retention within the ischemic tissue. To investigate this hypothesis, we performed intramuscular injections of iPSC-ECs into the ischemic limb of non-obese diabetic severe combined immune deficient (NOD SCID) mice immediately following ligation of the femoral artery using either PBS or SHIELD-2.5 (*i.e.*, the best performing SHIELD formulation in *in vitro* studies). Additional treatment groups included cell-free delivery of PBS alone and SHIELD-2.5 alone. For *in vivo* testing, iPSC-ECs were encapsulated in SHIELD-2.5 within a 1 mL syringe barrel prior to ejection through a 28 G syringe needle, similar to *in vitro* studies. All syringes were flushed with 0.1% bovine serum albumin prior loading and payload delivery to the ischemic limb to inhibit cellular retention within the syringe. Following transplantation into the ischemic limb, the iPSC-ECs were detected by BLI for up to 14 days (Fig. 4A) to monitor cell localization and survival. Bioluminescence

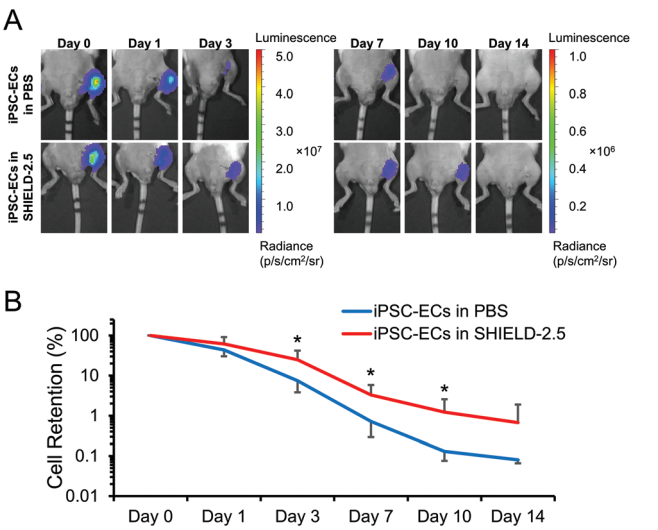

Fig. 4 Localization and survival of iPSC-ECs in the ischemic limb. (A) iPSC-ECs were delivered in PBS or SHIELD-2.5 by intramuscular injection of the ischemic limb and were tracked non-invasively by BLI for up to 14 days. (B) Percentage of injected cells retained in the ischemic limb. *$p < 0.05$, $n = 7$ (iPSC-ECs in PBS), $n = 9$ (iPSC-ECs in SHIELD-2.5).

imaging is a sensitive, non-invasive method to track metabolically active cells *in vivo* over time.[32,33] Consistent with previous studies,[6,21] following injection, there was a gradual decline in the bioluminescence signal (Fig. 4B). The quantification of the bioluminescence signal indicated a significant improvement in cell retention for iPSC-ECs encapsulated in SHIELD-2.5. On day 3, we observed 7% cell retention for cells delivered in PBS compared to 25% for cells encapsulated in SHIELD-2.5. Additionally, we observed an approximately tenfold greater survival of iPSC-ECs delivered in SHIELD-2.5 compared to PBS-mediated delivery at day 10. The persistence of the cells after 14 days was demonstrated histologically by green fluorescence protein (GFP) expression (Fig. S3†), although the cells did not appear to incorporate into existing vessels, and suggested a paracrine mechanism of inducing neovascularization.

In regions of ischemic injury, tissue damage is often accompanied by an inflammatory response as demonstrated in atherosclerotic patients[34–37] and several preclinical models of peripheral ischemia.[38,39] As such, it is possible that *in vivo* inflammation may result in the clearance of our exogenous cell-therapy, leading to reduced bioluminescence signal post-transplantation, in contrast to the proliferation observed in the *in vitro* environment. We hypothesize that the enhanced retention of iPSC-ECs transplanted in SHIELD-2.5 compared to saline-mediated delivery may be a result of the hydrogel secondary crosslinking, resulting in reduced cell dispersal at the injection site and improved long-term cell viability in the ischemic tissue.

Clinically, it has been shown that improvements in *in situ* cell retention provide cell dose-dependent symptomatic relief.[40] Thus, the improved retention of cells led us to assess functional recovery of the ischemic tissue. Laser Doppler perfusion imaging (LDPI) was performed to monitor blood flow in the ischemic limb and determine the effects of iPSC-EC transplantation on hind limb reperfusion. The quantification of the mean perfusion ratio indicated partial blood perfusion recovery in all treatment groups (Fig. S2†) without a statistically significant difference between the groups. The heterogeneity in the laser Doppler data as a result of breathing movement and slight differences in the orientation of the legs during imaging may contribute to the lack of statistical significance. Therefore, in addition to LDPI, we also performed the quantitative assessment of neovascularization by histological analysis and quantification.

The transplantation of iPSC-ECs has been shown to enhance microvessel formation to aid in tissue recovery following an ischemic insult.[6] To determine whether the improvement in iPSC-EC retention following delivery in SHIELD-2.5 would improve capillary formation in the ischemic hind limb, tissue explants from the ischemic limb were collected and stained for CD31 to quantify capillary density in each treatment group. CD31 staining demonstrated that treatment with iPSC-ECs delivered in SHIELD-2.5 (1020 ± 47 capillaries per mm^2) or in PBS (962 ± 79 capillaries per mm^2) resulted in significantly higher capillary density, compared to control PBS

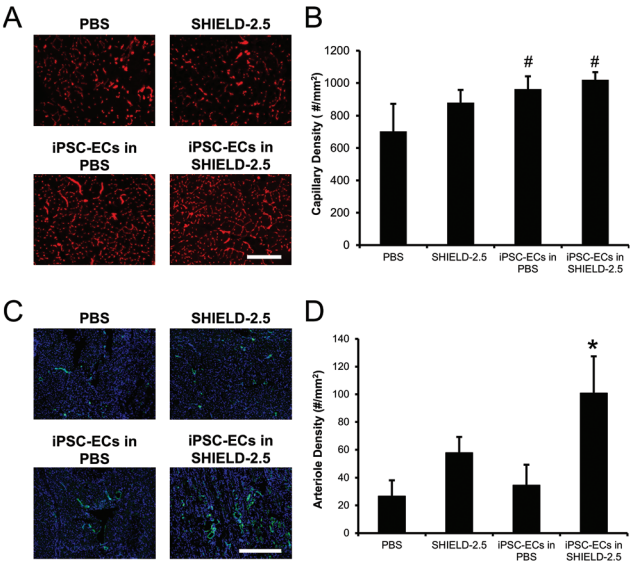

Fig. 5 Neovascularization in the ischemic limbs of mice receiving iPSC-ECs after 14 days. (A) Histological analysis of capillary density by immunofluorescent CD31 (red) staining of tissue sections from mice treated with saline, SHIELD-2.5, iPSC-ECs delivered in saline, or iPSC-ECs delivered in SHIELD-2.5. (B) Quantification of capillary density in the ischemic limbs. $^{\#}p < 0.05$ compared to PBS alone control group, $n = 4$. (C) Histological analysis of arteriole density by immunofluorescence staining of α-smooth muscle actin (α-SMA, green) and Hoechst 33342 nuclear dye (blue) in tissue sections from mice treated with saline, SHIELD-2.5, iPSC-ECs delivered in saline, or iPSC-ECs delivered in SHIELD-2.5. (D) Quantification of arteriole density in the ischemic limbs. $^{*}p < 0.05$ compared to all other treatment groups, $n = 5$. Scale bars: 200 μm (A), 500 μm (C).

treatment (802 ± 84 capillaries per mm^2) (Fig. 5A, $p < 0.05$). To further investigate the expanding vasculature following treatment, we next quantitatively assessed the arteriole density by immunostaining for α-SMA in each treatment group. Our studies demonstrated that treatment with iPSC-ECs delivered in SHIELD-2.5 resulted in significantly greater arteriole density (100 ± 26 arteries per mm^2), compared to the iPSC-ECs delivered in PBS (34 ± 14 arteries per mm^2) or SHIELD-2.5 alone (57 ± 11 arteries per mm^2) and PBS alone (26 ± 11 arteries per mm^2) controls (Fig. 5B). Therefore, these histological results indicate that the treatment of iPSC-ECs in SHIELD could significantly improve the arteriole density.

Our findings are consistent with those of prior studies, which found that shear-thinning hydrogels can improve cell survival during injection into sites of ischemic insult.[22,41,42] Additionally, the reinforcing network formed by the PNIPAM phase transition may reduce cell dispersal at the target site to further contribute to a higher cell viability and downstream neovascularization in the ischemic limb. Although capillary density and blood perfusion were not significantly improved, the significant increase in the arteriole density suggests that delivery of iPSC-ECs within SHIELD-2.5 could improve the formation of larger microvessels, which is important in neovascularization. As such, the biomaterial platform used in this study

may overcome the limitations of current cell-based therapies for transplantation into ischemic tissue.

Experimental

Materials synthesis

SHIELD is a two-component hydrogel consisting of (1) an engineered protein (termed C7) containing seven CC43 WW domains (denoted as C) and (2) an 8-arm polyethylene glycol (PEG) modified with proline rich peptides (denoted as P1). Alternatively, poly(*N*-isopropylacrylamide) (PNIPAM) is tethered to one or two arms on average of the 8-arm PEG, while the remaining arms are modified with P1 peptides. All chemicals for SHIELD synthesis were purchased from Sigma-Aldrich (Milwaukee, WI) unless otherwise noted. PEG-P1-PNIPAM copolymers were synthesized as described previously.[19,20] Briefly, peptide P1 (EYPPYPPPPYPSGC, M_w 1563 g mol^{-1}) was purchased through custom peptide synthesis from Genscript Corp (Piscataway, NJ, USA). Eight-arm polyethylene glycol vinyl sulfone (8-arm PEG-VS, M_w 20 000 g mol^{-1}) was purchased from Nanocs (Boston, MA). PNIPAM endcapped with a thiol group (PNIPAM-SH) (M_w 11 400 g mol^{-1} or 30 400 g mol^{-1}) was synthesized using Reversible Addition–Fragmentation chain Transfer (RAFT) polymerization and conjugated to the 8-arm PEG-VS *via* a Michael-type addition. The stoichiometry of the conjugation reaction was altered to modify on average either one or two arms of the PEG-VS as confirmed by ^{1}H NMR (Fig. S4†). Unreacted arms of PEG-VS were further reacted with excess P1 peptide.

The recombinant C7 protein (see Table S1† for full amino acid sequences) was cloned, synthesized, and purified as reported previously.[13] Briefly, the DNA sequence encoding the C7 linear protein was cloned into the pET-15b vector (Novagen) and transformed into BL21(DE3) pLysS *Escherichia coli* host strain (Life Technologies). The protein was expressed following isopropyl β-D-1-thiogalactopyranoside induction, purified by affinity chromatography *via* the specific binding of an N-terminal polyhistidine tag to Ni-nitrilotriacetic acid resin (Qiagen), dialyzed against phosphate buffered saline (PBS), and concentrated by diafiltration across Amicon Ultracel filter units (Millipore).

Hydrogel preparation

Each WW domain in C7 was treated as one C unit, and each pendant P1 peptide was treated as one P unit. All SHIELD formulations were designed to have a final C : P ratio of 1 : 1 and a 10% w/v of the total polymer in PBS. The weight percentage of the PNIPAM component was used to name five SHIELD formulations from SHIELD-0 to SHIELD-4, with 0 wt% to 4 wt% PNIPAM, respectively. SHIELD-0 was formed by mixing C7 and the PEG-P1 copolymer. SHIELD-1, SHIELD-2.5, and SHIELD-4 were formed by mixing C7 with the appropriate PEG-P1-PNIPAM copolymer (see Table S2†). SHIELD-1.25 was formed by mixing C7 with a blend of PEG-P1 and PEG-P1-PNIPAM at a 1 : 1 ratio.

Rheological characterization

Dynamic oscillatory rheology experiments were performed on a stress-controlled rheometer (AR-G2, TA instrument, New Castle, DE) using a 20 mm diameter cone-plate geometry. Samples were loaded immediately onto the rheometer after mixing, and a humidity chamber was secured in place to prevent dehydration. Frequency sweeps from 0.1–20 Hz at 22 °C and 37 °C were performed at 5% constant strain to obtain storage (G') and loss (G'') moduli. Shear-thinning and self-healing properties of the gel samples were characterized by measuring linear viscosity (γ) under a time sweep mode at alternating low and high shear rates of 0.1 s^{-1} and 10 s^{-1}, respectively, for 30 s each and a total of 150 s at 22 °C ($n \geq 3$).

Generation and characterization of iPSC-ECs

Human iPSCs (HUF5) were derived by retroviral-mediated transduction of Oct-4, Sox-2, Klf4, and c-Myc in healthy adult human dermal fibroblasts.[6] Endothelial differentiation of the iPSCs was performed based on our previous studies.[21] In brief, the iPSCs were dissociated in collagenase to form embryoid bodies in ultralow adhesion dishes in the presence of a differentiation medium that consisted of α-minimum Eagle's medium, 20% fetal bovine serum, L-glutamine, β-mercaptoethanol (0.05 mmol L^{-1}), 1% non-essential amino acids, bone morphogenetic protein-4 (BMP-4, 50 ng mL^{-1}, Peprotech), and vascular endothelial growth factor (VEGF-A, 50 ng mL^{-1}, Peprotech). After four days, the cells were reattached to gelatin-coated dishes in the same medium but lacking BMP-4. After 14 days, the iPSC-ECs were purified by fluorescence activated cell sorting based on the expression of CD31. In some experiments, the cells were further transduced with a firefly luciferase reporter gene as previously reported[6] for non-invasive tracking by bioluminescence imaging (BLI).

In vitro cell encapsulation, injection, and quantification of viability

The iPSC-ECs were cultured in EGM-2MV growth medium (Lonza) and kept in a humidified, 5% CO_2 environment at 37 °C with medium changes every 2 days. The cells were expanded and passaged using TrypLE Express (Invitrogen). *In vitro* viability and proliferation experiments were performed with 30 μL gel volume containing 5 × 10^4 cells. The cell suspension was first mixed with C7 to yield a 10% w/v suspension in PBS before further mixing with the 8-arm PEG-P1-PNIPAM copolymer solution. The volumes of the C7 cell suspension and PEG-P1-PNIPAM solution were adjusted to achieve a final C : P ratio of 1 : 1 at a total cell-laden hydrogel concentration of 10% w/v for all formulations. For cell injection studies, the final mixing step with PEG-P1-PNIPAM was performed in the barrel of a 1 mL insulin syringe fitted with a 28 G needle. The mixture was allowed to gel for 5 min before injecting into a circular silicone mold (diameter = 4 mm, height = 2.5 mm) within a 24-well plate using a syringe pump (SP220I; World Precision Instruments) at a flow rate of 1 mL min^{-1}. Cell viability was determined using a LIVE/DEAD viability/cytotoxicity

kit (Invitrogen) immediately post-injection. Cell proliferation under hypoxia was conducted by encapsulating iPSC-ECs in SHIELD, injecting into silicone molds as described above, and then incubating in a hypoxia chamber (1% O_2, 5% CO_2, and 94% N_2) with EGM-2MV medium. DNA quantification was performed using the Quant-iT PicoGreen dsDNA Assay Kit (Thermo Fisher) at days 0, 1, 4, 7, and 14 post-injection ($n \geq 3$), according to the manufacturer's instructions.

Immunofluorescence staining for cell spreading

Cells were fixed with 4% paraformaldehyde, permeabilized with 0.2% Triton X-100 solution in PBS, and stained with an antibody targeting CD31 (1 : 200 dilution, Abcam) with a goat anti-mouse secondary antibody conjugated to a 488 nm Alexa Fluor fluorophore (1 : 200 dilution, ThermoFisher). Samples were counter-stained with rhodamine phalloidin (1 : 300 dilution, Life Technologies) and 4′,6-diamidino-2-phenylindole (DAPI, 1 μg mL^{-1}, Life Technologies). Images were collected using a Leica confocal microscope by creating *z*-stacks of greater than 200 μm depth with 2.4 μm intervals between slices in the middle of the hydrogel. Representative images shown are maximum projections.

Growth factor secretion in hypoxia

The iPSC-ECs were injected into ultra-low attachment 96-well plates (Corning) within a 50 μL gel volume of SHIELD-0 or SHIELD-2.5 containing 5×10^5 cells (n = 4 hydrogels per group). The cells were further cultured in hypoxia (1% O_2) or normoxia (20% O_2) as a control in EBM-2 with 2% FBS. Angiogenic growth factor secretion was quantified using an angiogenesis antibody array (Human Angiogenesis Proteome Profiler antibody array, R&D systems) according to the manufacturer's protocol. Briefly, the conditioned iPSC-EC medium was collected 4 days post-injection and was pooled, passed through 0.2 μm sterile filters, and incubated with the assay-specific antibody cocktail for 1 hour at room temperature. Nitrocellulose membranes, containing the capture antibodies, were blocked using the assay-specific blocking solution. Thereafter, the sample/detection antibody cocktail mixture was added to the membranes and incubated overnight at 4 °C on a rocking platform. Each membrane was washed three times with 1× wash buffer for 10 min on a rocking platform before incubation with streptavidin–horseradish peroxidase (1 : 2000 dilution, R&D systems) for 30 min at room temperature. The membranes were then washed three times with 1× wash buffer for 10 min prior to incubation with the assay-specific Chemi Reagent Mix. The membranes were exposed to X-ray film for 3 minutes. Histogram profiles for selected analytes were generated by quantifying densitometry using Image J software, and the results were confirmed in two independent experiments.

Hind limb ischemia

All animal procedures were performed in accordance with the Guidelines for Care and Use of Laboratory Animals of Stanford University and approved by the Administrative Panel on Laboratory Animal Care of Stanford University. In the anesthetized state, unilateral hind limb ischemia was induced in male, 3-month old NOD SCID mice by ligation and excision of the left femoral artery as previously reported.[21,43,44] The right limb served as the non-ischemic control. Immediately following ischemia induction, mice were randomly assigned to receive a 20 μL intramuscular (IM) injection in the gastrocnemius muscle of the following treatment groups: (1) PBS (n = 14); (2) SHIELD-2.5 (n = 13); (3) 1×10^6 iPSC-ECs in PBS (n = 7); and (4) 1×10^6 iPSC-ECs in SHIELD-2.5 (n = 9). To assess cell survival and location, animals were injected intraperitoneally with D-luciferin (150 μg mL^{-1}), and BLI was performed with an IVIS imaging system (Xenogen Corp.). Data were acquired using Living Image software (Xenogen Corp.) and expressed in units of average radiance (p s^{-1} cm^{-2} sr^{-1}). Additionally, relative blood perfusion recovery was assessed by laser Doppler spectroscopy, as described previously,[44,45] and expressed as the mean perfusion ratio (perfusion of ischemic limb)/(perfusion of contralateral unoperated limb).

Arteriole and capillary density analysis

After 14 days, the animals were euthanized, and the ischemic gastrocnemius muscle was flash-frozen in O.C.T. compound embedding medium for histological assessment. Frozen tissues were cryosectioned into 10 μm transverse sections, and representative tissue sections were stained with hematoxylin and eosin (H&E) to visualize the tissue morphology. To determine the arteriole density, cryosections of the ischemic gastrocnemius muscle were immunofluorescently stained with the anti-α-smooth muscle actin (α-SMA) (1 : 400 dilution, Sigma) monoclonal primary antibody, followed by the Alexa Fluor 488 goat-anti mouse (1 : 200 dilution, Fisher Scientific) secondary antibody, and nuclei were stained using Hoechst 33342.[6,46,47] For capillary density, sections were stained with anti-CD31 (1 : 100 dilution, Agilent Dako), followed by Alexa Fluor 594 goat-anti mouse secondary antibody.[6,45] Four separate tissue sections were analyzed for each animal. For each tissue section, three representative images were acquired with a 10× objective using a fluorescence microscope (Keyence, BZ-X710). The number of α-SMA positive vessels was counted and then averaged among each tissue section and was then expressed as arteriole density (#arterioles per mm^2). Similarly, the number of CD31-positive vessels was counted and then averaged among each tissue section and was then expressed as capillary density (# capillaries per mm^2). To visualize iPSC-ECs within the tissue sections, the Alexa Fluor-594-conjugated GFP antibody (Fisher Scientific) was stained on tissue sections. Confocal imaging confirmed positive GFP staining based on endogenous GFP expression as well as expression based on GFP antibody staining.

Statistical analysis

All data are presented as mean ± standard deviation. For all *in vitro* assays, statistical significance was calculated between groups using a one-way ANOVA followed by a Tukey *post hoc*

test. For preclinical *in vivo* studies, ANOVA with Bonferroni adjustment was employed. Values were considered to be significantly different when the p value was <0.05.

Conclusions

In summary, we report a physically crosslinked hydrogel with tunable *in situ* mechanics for the treatment of ischemic injury and disease. Our results showed that the SHIELD family of hydrogels provides acute protection from membrane damage during injection. Additionally, we demonstrated that SHIELD with an intermediate *in situ* stiffness range of 200–400 Pa (SHIELD-2.5) could significantly improve iPSC-EC *in vitro* viability, compared to other stiffness values. Furthermore, SHIELD-2.5 improved cell retention and arteriogenesis in a murine model of PAD. This approach may be useful for minimizing the number of cell administrations required to promote neovascularization in the ischemic tissue.

Conflicts of interest

There are no conflicts to declare.

Acknowledgements

The authors acknowledge funding support from the National Institutes of Health (R21-EB020235 to S. C. H. and N. F. H; R00-HL098688 and R01-HL127113 to N. F. H.; and T32-HL098049-06 to A. F.). S. C. H. was also supported by funding from the Stanford Bio-X (IIP-7-75), CIRM (RT3-07948), and Coulter Foundation (CP-2014-4). The authors thank Dr Laura Marquardt for assistance with recombinant protein purification and Dr Chris Madl for assistance with proteome secretion studies.

References

1 F. G. Fowkes, D. Rudan, I. Rudan, V. Aboyans, J. O. Denenberg, M. M. McDermott, P. E. Norman, U. K. Sampson, L. J. Williams, G. A. Mensah and M. H. Criqui, *Lancet*, 2013, **382**, 1329–1340.

2 D. Mozaffarian, E. J. Benjamin, A. S. Go, D. K. Arnett, M. J. Blaha, M. Cushman, S. R. Das, S. de Ferranti, J.-P. Després, H. J. Fullerton, V. J. Howard, M. D. Huffman, C. R. Isasi, M. C. Jiménez, S. E. Judd, B. M. Kissela, J. H. Lichtman, L. D. Lisabeth, S. Liu, R. H. Mackey, D. J. Magid, D. K. McGuire, E. R. Mohler, C. S. Moy, P. Muntner, M. E. Mussolino, K. Nasir, R. W. Neumar, G. Nichol, L. Palaniappan, D. K. Pandey, M. J. Reeves, C. J. Rodriguez, W. Rosamond, P. D. Sorlie, J. Stein, A. Towfighi, T. N. Turan, S. S. Virani, D. Woo, R. W. Yeh and M. B. Turner, *A Report From the American Heart Association*, 2015,DOI: 10.1161/cir.0000000000000350.

3 D. J. Collinson and R. Donnelly, *Eur. J. Vasc. Endovasc. Surg.*, 2004, **28**, 9–23.

4 Z. Raval and D. W. Losordo, *Circ. Res.*, 2013, **112**, 1288–1302.

5 Z. E. Clayton, G. S. Yuen, S. Sadeghipour, J. D. Hywood, J. W. Wong, N. F. Huang, M. K. Ng, J. P. Cooke and S. Patel, *Int. J. Cardiol.*, 2017, **234**, 81–89.

6 A. J. Rufaihah, N. F. Huang, S. Jamé, J. C. Lee, H. N. Nguyen, B. Byers, A. De, J. Okogbaa, M. Rollins, R. Reijo-Pera, S. S. Gambhir and J. P. Cooke, *Arterioscler., Thromb., Vasc. Biol.*, 2011, **31**, e72–e79.

7 H. Lawall, P. Bramlage and B. Amann, *J. Vasc. Surg.*, 2011, **53**, 445–453.

8 B. A. Aguado, W. Mulyasasmita, J. Su, K. J. Lampe and S. C. Heilshorn, *Tissue Eng., Part A*, 2012, **18**, 806–815.

9 L. M. Marquardt and S. C. Heilshorn, *Curr. Stem Cell Rep.*, 2016, **2**, 207–220.

10 A. A. Foster, L. M. Marquardt and S. C. Heilshorn, *Curr. Opin. Chem. Eng.*, 2017, **15**, 15–23.

11 C. B. Rodell, A. L. Kaminski and J. A. Burdick, *Biomacromolecules*, 2013, **14**, 4125–4134.

12 C. Yan, M. E. Mackay, K. Czymmek, R. P. Nagarkar, J. P. Schneider and D. J. Pochan, *Langmuir*, 2012, **28**, 6076–6087.

13 A. Parisi-Amon, W. Mulyasasmita, C. Chung and S. C. Heilshorn, *Adv. Healthcare Mater.*, 2013, **2**, 428–432.

14 P. Lu, K. Takai, V. M. Weaver and Z. Werb, *Cold Spring Harbor Perspect. Biol.*, 2011, **3**, a005058.

15 F. Trensz, F. Lucien, V. Couture, T. Söllrald, G. Drouin, A. J. Rouleau, M. Grandbois, G. Lacraz and G. Grenier, *Skeletal Muscle*, 2015, **5**, 5.

16 W. Sun, N. A. Kurniawan, A. P. Kumar, R. Rajagopalan and C. T. Lim, *Cell. Mol. Bioeng.*, 2014, **7**, 205–217.

17 A. D. Doyle, N. Carvajal, A. Jin, K. Matsumoto and K. M. Yamada, *Nat. Commun.*, 2015, **6**, 8720.

18 F. P. Seib, M. Prewitz, C. Werner and M. Bornhäuser, *Biochem. Biophys. Res. Commun.*, 2009, **389**, 663–667.

19 L. Cai, R. E. Dewi, A. B. Goldstone, J. E. Cohen, A. N. Steele, Y. J. Woo and S. C. Heilshorn, *Adv. Healthcare Mater.*, 2016, **5**, 2758–2764.

20 L. Cai, R. E. Dewi and S. C. Heilshorn, *Adv. Funct. Mater.*, 2015, **25**, 1344–1351.

21 W. Mulyasasmita, L. Cai, R. E. Dewi, A. Jha, S. D. Ullmann, R. H. Luong, N. F. Huang and S. C. Heilshorn, *J. Controlled Release*, 2014, **191**, 71–81.

22 A. C. Gaffey, M. H. Chen, C. M. Venkataraman, A. Trubelja, C. B. Rodell, P. V. Dinh, G. Hung, J. W. MacArthur, R. V. Soopan, J. A. Burdick and P. Atluri, *J. Thorac. Cardiovasc. Surg.*, 2015, **150**, 1268–1276.

23 S. Lin, N. Sangaj, T. Razafiarison, C. Zhang and S. Varghese, *Pharm. Res.*, 2011, **28**, 1422–1430.

24 X. Liang, Y. Ding, Y. Zhang, H. F. Tse and Q. Lian, *Cell Transplant.*, 2014, **23**, 1045–1059.

25 P. R. Baraniak and T. C. McDevitt, *Regener. Med.*, 2010, **5**, 121–143.

26 K. Lee, E. A. Silva and D. J. Mooney, *J. R. Soc., Interface*, 2011, **8**, 153–170.
27 H. K. Awada, N. R. Johnson and Y. Wang, *J. Controlled Release*, 2015, **207**, 7–17.
28 I. L. Kim, C. G. Pfeifer, M. B. Fisher, V. Saxena, G. R. Meloni, M. Y. Kwon, M. Kim, D. R. Steinberg, R. L. Mauck and J. A. Burdick, *Tissue Eng., Part A*, 2015, **21**, 2680–2690.
29 C. Murdoch, A. Giannoudis and C. E. Lewis, *Blood*, 2004, **104**, 2224–2234.
30 M. E. Kroon, P. Koolwijk, B. van der Vecht and V. W. van Hinsbergh, *Blood*, 2000, **96**, 2775–2783.
31 W. H. Lai, J. C. Ho, Y. C. Chan, J. H. Ng, K. W. Au, L. Y. Wong, C. W. Siu and H. F. Tse, *PLoS One*, 2013, **8**, e57876.
32 C. H. Contag and B. D. Ross, *J. Magn. Reson. Imaging*, 2002, **16**, 378–387.
33 Y. A. Cao, M. H. Bachmann, A. Beilhack, Y. Yang, M. Tanaka, R. J. Swijnenburg, R. Reeves, C. Taylor-Edwards, S. Schulz, T. C. Doyle, C. G. Fathman, R. C. Robbins, L. A. Herzenberg, R. S. Negrin and C. H. Contag, *Transplantation*, 2005, **80**, 134–139.
34 N. Fiotti, C. Giansante, E. Ponte, C. Delbello, S. Calabrese, T. Zacchi, A. Dobrina and G. Guarnieri, *Atherosclerosis*, 1999, **145**, 51–60.
35 F. B. Smith, A. J. Lee, C. M. Hau, A. Rumley, G. D. Lowe and F. G. Fowkes, *Blood Coagulation Fibrinolysis*, 2000, **11**, 43–50.
36 M. Montagnana, C. Fava, E. Arosio, M. Degan, R. M. Tommasoli, S. De Marchi, P. Delva, R. Spadaro, G. C. Guidi, A. Lechi, C. L. Santonastaso and P. Minuz, *Int. J. Angiol.*, 2007, **16**, 84–88.
37 Y. Iwashima, T. Horio, Y. Suzuki, S. Kihara, H. Rakugi, K. Kangawa, T. Funahashi, T. Ogihara and Y. Kawano, *Atherosclerosis*, 2006, **188**, 384–390.
38 D. Scholz, T. Ziegelhoeffer, A. Helisch, S. Wagner, C. Friedrich, T. Podzuweit and W. Schaper, *J. Mol. Cell. Cardiol.*, 2002, **34**, 775–787.
39 P. K. Shireman, *J. Vasc. Surg.*, 2007, **45**(Suppl A), A48–A56.
40 D. H. Walter, H. Krankenberg, J. O. Balzer, C. Kalka, I. Baumgartner, M. Schluter, T. Tonn, F. Seeger, S. Dimmeler, E. Lindhoff-Last and A. M. Zeiher, *Circ.: Cardiovasc. Interventions*, 2011, **4**, 26–37.
41 C. Loebel, C. B. Rodell, M. H. Chen and J. A. Burdick, *Nat. Protoc.*, 2017, **12**, 1521–1541.
42 C. B. Rodell, J. W. MacArthur, S. M. Dorsey, R. J. Wade, L. L. Wang, Y. J. Woo and J. A. Burdick, *Adv. Funct. Mater.*, 2015, **25**, 636–644.
43 H. Niiyama, N. F. Huang, M. D. Rollins and J. P. Cooke, *J. Visualized. Exp.*, 2009, **23**, e1035.
44 K. H. Nakayama, G. Hong, J. C. Lee, J. Patel, B. Edwards, T. S. Zaitseva, M. V. Paukshto, H. Dai, J. P. Cooke, Y. J. Woo and N. F. Huang, *ACS Nano*, 2015, **9**, 6900–6908.
45 G. Hong, J. C. Lee, A. Jha, S. Diao, K. H. Nakayama, L. Hou, T. C. Doyle, J. T. Robinson, A. L. Antaris, H. Dai, J. P. Cooke and N. F. Huang, *Circ. Cardiovasc. Imaging*, 2014, **7**, 517–525.
46 N. F. Huang, H. Niiyama, C. Peter, A. De, Y. Natkunam, F. Fleissner, Z. Li, M. D. Rollins, J. C. Wu, S. S. Gambhir and J. P. Cooke, *Arterioscler., Thromb., Vasc. Biol.*, 2010, **30**, 984–991.
47 N. F. Huang, A. Lam, Q. Fang, R. E. Sievers, S. Li and R. J. Lee, *Regener. Med.*, 2009, **4**, 527–538.

